Asian Journal of Chemistry; Vol. 34, No. 8 (2022), 2147-2154

ASIAN JOURNAL OF CHEMISTRY

https://doi.org/10.14233/ajchem.2022.23880

Berberine Loaded Magnetic Nanoparticles for Breast Cancer Therapy on MDA-MB-231 Cells Lines

A. VENKATA SATYA MADHULATHA and C. RONALD DARWIN*

Department of Pharmacology, School of Pharmaceutical Sciences, Vels Institute of Science, Technology and Advanced Studies, Chennai-600117, India

*Corresponding author: E-mail: ronaldpharma@gmail.com

Received: 24 April 2022; *Accepted*: 6 June 2022; *Published online*: 18 July 2022; AJC-20901

Berberine is an alkaloid naturally-derived from *Berberis aristata* and a family *Berberidaceae* exhibits a broad spectrum of pharmacological benefits, including antiviral and anticancer properties. The recent development of nanomedicine is an art of delivering drugs to the target-site by improving their safety and efficacy. In present study, four berberine-loaded magnetic nanoparticles (BBR/MNPs) were prepared using a modified co-precipitation method with calcination. The resulting BBR/MNPs were characterized by FTIR, XRD, HRSEM, zeta potential, VSM, loading efficiency, stability and *in vitro* release studies. The most proven magnetic nanoparticles formulation type in dissolution was followed by *in vitro* anticancer studies on MDA-MB-231 cells. XRD, FTIR and TGA results proved that the formed BBR/MNPs were ordered in their structure with iron, silanol groups and berberine moieties. The HRSEM reported the average particle size of MNPs varies from 100 to 250 nm after loading with berberine also had a regular spherical shape. The value of the zeta potential was -9 mV and 15 mV at pH 6 for bare MNPs and BBR/MNPs, respectively. Loading efficiency and stability were good at BBR/MCM-41MNP. The saturated magnetization (Ms) value of Fe-MCM-41 MNP (81.76 emu/g) was obtained by VSM analysis. *In vitro* dissolution studies of four BBR/MNPs at a three different pH 5.5, 6.5, 7.4 including BBR/MCM-41 MNP were 86%, 84% and 82%, respectively. *In vitro* anticancer studies with BBR/MCM-41-MNP on treated MDA-MB-231 breast cancer cells in comparison to standard doxorubicin. The MTT assay confirmed the cytotoxic effect of BBR/MCM-41-MNP *in vitro*. The resulting data were statistically analyzed using one-way Anova analysis with N = 3 replicates. The IC_{50} values (mean standard deviation) of BBR, BBR/MCM-41 MNP and standard doxorubicin were obtained as 16.754 ± 0.651, 6.750 ± 0.048, 4.955 ± 0.042 µg/mL with significant $p < 0.0001$. The best result was BBR/MCM-41 MNP with an average particle size 50 nm, which showed good drug loading efficiency and size stability above 7 days. Drug release was maximal (86%) at pH 5.5. The MTT-assay confirmed that BBR/MCM-41MNP exhibited more cytotoxicity on MDA-MB-231 cells than BBR, MCM-41MNP. The IC_{50} of BBR/MCM-41 was closed that of standard doxorubicin. The BBR/MCM-41MNP showed the optimum drug release with potent anticancer activity along with magnetic targeting.

Keywords: Berberine, Magnetic nanoparticles, Loading efficiency, Release study, Anticancer study.

INTRODUCTION

Globally, cancer is the second largest cause of death with an estimated 9.9 million deaths or one in six deaths, in the year 2020 [1]. In men lung, prostate, colon, stomach and liver cancer were the most common cancer types. On the other side, women were highly affected by breast, colon, lung, cervical and thyroid cancers. Breast cancer is very common type of cancer in women, occurring 85% at the mucosal epithelium of the milk ducts and 15% at the lobules of glandular tissue in the breast [2]. The early stage of cancerous growth is limited to the ducts or lobules called *in situ* [3-5]. Upon time the *in situ* type cancers can develop into invasive breast cancer and then spread to regional metastases or surrounding organs in the body (distant metastases). In 2020 global statistical year, 2,261,419 women were affected by cancer while 684,996 women died of cancer. In India, 3,465,951 women were morbid due to cancer and 1,121,413 women were mortal due to it. Treatment for breast cancer generally combines amputation, radiation therapy and anticancer drugs (hormone therapy, chemotherapy and/or targeted biological therapy) to treat the cancer. However, the treatment carries life-threatening side effects [6-8]. The anticancer activity can be evaluated both *in vitro* and *in vivo* in comparison to a standard drug on MDA-MB-231cells.

Nanoparticles are submicron ranged (100-1000 nm) microscopic particles that are usually composed of materials such as polymers, phospholipids, inorganic salts, *etc.* [9]. There are several kinds of nanoparticles with varying size, shape, composition and functionalities. They may contain liposomes, polymeric, iron salts, gold, quantum specks, *etc.* Among the types of nanoparticles, magnetic nanoparticles are a specially designed system that delivers the drug to its desired site with the help of a magnetic field. The magnetic property was obtained by the core of the nanoparticle, which consists of metals such as cobalt, iron, nickel, *etc.* [10-12]. Magnetic nanoparticles are attractive because they can load large amounts of drug molecules into their pores and eventually release them at the cellular level. Owing to their less toxicity, biocompatibility and high stability, the iron oxide containing magnetic nanoparticles (MNPs) have unique clinical applications.

Natural herbal medicines have a multifaceted role in the prevention, diagnosis and treatment of ailments. During use, natural medicines show low side effects, low toxicity and more compatibility with all polymers used in the preparations. But it has some problems with low stability and low bioavailability. Berberine (BBR) belongs to isoquinoline alkaloids, extracted from various parts like root, rhizome, stem and bark of herbs such as *Berberis aristata* and *Berberis vulgaris* [13-15]. Active berberine components have shown diversified pharmacological uses, including anti-inflammatory, antilipidemic and antidepressant and effects, treatment of diabetics and control of cardiovascular diseases, anticancer and antimicrobial properties.

In present work, the fabrication of mesoporous magnetic particles was performed using a modified co-precipitation method. The formed magnetic nanoparticles were synthesized and confirmed by FTIR, XRD and TGA to identify the optimal size, structural arrangement of the nanoparticles and thermal stability of magnetic nanoparticles. All the four berberine-loaded magnetic nanoparticles (BBR/MNPs) were prepared were then measured for their percent drug release, stability and colloidal potency. Finally, the compounds was screened by (3-(4,5-dimethylthiazol-2-yl)-2,5-diphenyl tetrazolium bromide) MTT assay on MDA-MB-231 treated cells and the percent cell viability and IC_{50} value with mean and SD were calculated. A statistical study was performed by one-way Anova analysis using three numbers of replicates.

EXPERIMENTAL

Berberine in the form of pure powder was received as a complimentary sample from Himalayan Herbaria Inc., India. Pluronic P123 ($EO_{20}PO_{70}EO_{20}$), tetra ethyl orthosilicate (TEOS, 98%), conc. HCl (48%), ethyl alcohol (> 99.9%), *n*-hexane and butanol were procured from Merck. Iron acetylacetone, cetyltrimethylammonium bromide (CTAB) and ammonium hydroxide was obtained from Sigma-Aldrich. All chemicals and polymers used were of analytical grade. MDA-MB-231 cell lines were obtained from Amala Cancer Institute, Kerala, India.

Synthesis of BBR/SiO_2

Step-1: Synthesis of SiO_2 mesoporous silica: SiO_2 mesoporous silica was prepared using a surfactant template, triblock co-polymer Pluronic P123 ($EO_{20}PO_{70}EO_{20}$) [16]. A typical composition in mole ratio was TEOS:Pluronic P 123:conc. HCl: H_2O:ethanol (1:0.00967:0.0012:185:8.7), respectively. Placed 1.4 g of Pluronic P123 in 4.0 mL of ethanol, then 5.2 g of tetra ethyl orthosilicate (TEOS) was added. To this solution, added 2.7 mL of 0.04 wt.% HCl, 6.0 mL of ethanol and the mixture was stirred overnight at 32 ºC. It was transferred to a Teflon bottle and heated and refluxed for 48 h at 100 ºC. The resultant precipitate was filtered, washed with double-deionized water and then dried. The intact surfactant layer was removed by calcinating at about 500 ºC for 8 h.

Step-2: Impregnation of magnetite into Fe-SiO_2 using iron(III) acetate as a precursor: Iron(III) acetylacetone (0.3153 g) was dissolved in 3 mL of acetone containing 0.3 mL of HNO_3 and stirred for 4 h at 80 ºC. SiO_2 particles (0.25 g) were suspended in $Fe(acetylac)_3$ solution overnight and the solvent removed by stirring for 4 h at 25 ºC. Then powder was heated up to 500 ºC in a furnace for 2 h with increasing temperature of 2 ºC/min.

Synthesis of BBR/MCM-41

Step-1: Synthesis of MCM-41 mesoporous silica: MCM-41 mesoporous silica was prepared by placing 2.4 g of cetyl trimethylammonium bromide (CTAB) in 120 mL of deionized water and stirred until the mixture was uniform and clear [17]. After adding 8 mL of NH_4OH, the resultant mixture was stirred for 5 min and then 10 mL of TEOS (98%) was added to the above surfactant solution and then stirred for 24 h at room temperature. The obtained white precipitate was washed with double-deionized water, collected and then dried. By calcinating at 500 ºC for 8 h, the surfactant template was removed.

Step-2: Impregnation of magnetite into MCM-41 using iron(III) acetate as precursor: Iron(III) acetylacetone (0.3153 g) dissolved in 3 mL of acetone with 0.3 mL of HNO_3 and stirred for 4 h at 80 ºC. 0.25 g of MCM-14 particles were suspended in $Fe(acetylac)_3$ solution overnight and the solvent removed by stirring for 4 h at room temperature. Then powder heated up to 500 ºC in a furnace for 2 h with increasing temperature of 2 ºC per min.

Synthesis of BBR/KIT-6

Step-1: Synthesis of KIT-6 mesoporous silica: KIT-6 mesoporous silica particles were synthesized using a triblock copolymer ($EO_{20}PO_{70}EO_{20}$) Pluronic P123 as the surfactant template. A typical composition in molar ratio found was TEOS: P123:HCl:H_2O: butanol (1.00:0.017:1.83:195:1.31), respectively. The surfactant Pluronic P123 (1.23 g) in a mixture of 44 g of water and 2.25 g of conc. HCl at 38-40 ºC. TEOS (98%) was then added to the above surfactant solution [18]. Then, it was stirred for 20 h at 32 ºC. After transferring the above reaction mass to a Teflon bottle; it was heated to 100 ± 2 ºC for 48 h. The white precipitate was filtered under vacuum, washed with double-deionized water and air-dried. By heating to 500 ºC for 8 h, the surfactant template was removed.

Step-2: Impregnation of magnetite into KIT-6 using iron(III) acetate as a precursor: Iron(III) acetylacetone (0.3153 g) was dissolved in 3 mL of acetone with 0.3 mL of

HNO_3 and stirred for 4 h at 80 ºC. The KIT-6 particles (0.25 g) were suspended in $Fe(acetylac)_3$ solution overnight and the solvent removed by stirring for 4 h at room temperature. Then powder heated up to 500 ºC in a furnace for 2 h with increasing temperature of 2 ºC per min.

Synthesis of BBR/SBA-15

Step-1: Synthesis of SBA-15 mesoporous silica: SBA-15 mesoporous silica particles were developed using a triblock Pluronic P123 ($EO_{20}PO_{70}EO_{20}$) copolymer as template surfactant [19]. Molar ratio was found to be TEOS:P123:conc. HCl:H_2O (1:0.017:2.9:202.6), respectively. To a mixture of water and conc. HCl at 32 ± 2 ºC, added the surfactant Pluronic P123. Added tetraethyl orthosilicate (98%) to the above surfactant solution, the mixture was stirred for 24 h at 30 ± 2 ºC. Transferred the resulting mixture into a Teflon bottle and heated to 100 ºC for 2 days. The white precipitate product was collected using filtration, washed with double-deionized water and air-dried by calcinating in air at 500 ºC for 8 h, the attached reminant surfactant template was removed.

Step-2: Impregnation of magnetite into SBA-15 using iron(III) acetate as precursor: Iron(III) acetylacetone (0.3153 g) was dissolved in 3 mL of acetone with 0.3 mL of conc. HNO_3 and stirred for 4 h at 80 ºC. Formed SBA-15 particles (0.25 g) were placed in a $Fe(acetylac)_3$ solution overnight and the solvent removed by stirring for 4 h at room temperature. Then powder heated up to 500 ºC in a furnace for 2 h with increasing temperature of 2 ºC per min. This sample was named as Fe–SBA-15.

Encapsulation of drug into magnetic nanoparticles: The prepared mesoporous Fe-SiO_2, Fe-MCM-41 and Fe-KIT-6 and Fe-SBA-15 samples (0.4 g) were taken individually and added to 20 mL of 1.4 g berberine-hexane solution and macerated for 3 days with stirring. Then the berberine-loaded magnetic nanoparticles were obtained by centrifugation, collecting the product by filtration using hexane washing. Then the materials were dried at 60 ºC for 10 h under vacuum.

Characterization of berberine loaded magnetic nanoparticles

Drug response study: Usually, UV-visible spectrophotometry is an important tool for studying the formation of MNPs in aqueous suspension [20]. The graph includes BBR, BBR/SiO_2, BBR/MCM-41, BBR/KIT-6 and BBR/SBA-15. The UV-vis spectrum of BBR and synthesized BBR-MNPs revealed that a new absorption peak at 403 nm.

FTIR analysis: Sample (0.2 g) were ground with 0.18 g of KBr powder and pressed to form a disc for FTIR scanning [21]. These pellets were analyzed in FTIR and then Data were collected at a wavenumber range of 4000-400 cm^{-1}.

X-ray diffraction (XRD) analysis: The XRD (X-ray diffractometer) (Shimadzu Analytical Ltd.) was performed for understand the behaviour of crystal structure of the synthesized magnetic nanoparticles.

Thermal analysis: Thermal gravimetric analysis (TGA) was performed in a nitrogen atmosphere using the SDTQ 600 instrument. The sample was placed in an aluminum pan and heated from room temperature (25 ºC) to 250 ºC at a heating rate of 10 ºC/min.

HRSEM analysis: Measurement of average diameter of nanoparticles was performed in deionized water by the dynamic light scattering technology [22] at room temperature (25 ºC) and morphology features of polymeric nanoparticles were studied using a scanning electron microscopy (SEM instrument S-4800).

Loading efficiency: UV-visible spectroscopy is used to estimate the content of berberine (drug) at a wavelength of 403 nm. It is used to calculate the drug loading, where W_0, W_1 and W_{NP} represents the initial weight of berberine, the weight of detected berberine in the solution and weight of the BBR-MNPs, respectively.

$$\text{Drug loading efficiency (\%)} = \frac{W_0 - W_1}{W_{NP}} \times 100$$

Colloidal stability of berberine magnetic nanoparticles: The stability of berberine loaded magnetic nanoparticles was determined by colloidal stability analysis, it was conducted for 7 days using DLS at 37 ºC, which mimics the physiological conditions. Samples were prepared with deionized water with an adjusted concentration at 1 mg/mL. Then, it was used to determine the colloidal stability of the particles.

$$\text{Colloidal stability } (t_n) = \frac{\text{Nanoparticle size } (t_n)}{\text{Initial nanoparticle size } (t_0)} \times 100$$

where colloidal stability of the particles in each day (t_n) is equaled to the nanoparticle size of each day (t_n) to the initial size of the nanoparticle at the first test (t_0).

Zeta potential (ζ): Measurement of zeta potential was identified by Zetameter. The zeta potential is the degree of repulsion between adjacent, similarly charged particles in any dispersion. Generally, an optimal zeta potential with small particle size decides the stability [23].

Vibrating sample magnetometer analysis: Vibrating sample magnetometer (VSM model) instrument used to estimate the magnetic properties of Fe-MCM-41 magnetic nanoparticles. The hysteresis curve obtained between applied magnetic field from -20000 to 20000 Oe on X-axis and magnetization (emu/g) on Y-axis.

***In vitro* dissolution study:** Three different dissolution media such as phosphate buffer solutions (PBS) pH 5.5, pH 6.5 and pH 7.4 were selected for *in vitro* dissolution studies [24]. According to the United States Pharmacopeia (USP) Method II (the paddle method), the bath volume for each medium was 900 mL at 37 ± 0.5 ºC and its rotational speed was 100 rpm [24]. Placed crude BBR (100 mg) and prepared BBR loaded MNPs into the dissolution vessels. A 5 mL of sample aliquot was removed at predetermined time intervals (*i.e.* 2 h, 4 h, 8 h, *etc*. up to 36 h) and filtered using Whatman filter paper No. 1. To maintain the sink conditions, same volume of fresh medium was replaced. The filtered samples were appropriately diluted and measured for their absorbance using a dual-beam spectrophotometer (Lab India UV/Visible Spectrophotometer, India) at a maximum wavelength of 403 nm.

***In vitro* cytotoxicity studies of berberine loaded MCM-41 MNPs:** The cytotoxicity study of berberine loaded MCM-41 MNPs was performed on selected breast cancer cells named

MDA-MB-231 determined by cell proliferation assay with MTT Reagent. The cytotoxic effects of free MNP MCM-41, BBR and BBR/MCM-41 were evaluated on breast cancer cells *i.e.*, MDA-MB-231 using 3-(4,5-dimethylthialzol-2-yl)-2,5-diphenyl tetrazolium bromide (MTT) assay methods [25]. The MDA-MB-231 cells were treated by free MNP MCM-41, BBR and BBR/MCM-41 at different concentrations ranging from 0-40 µg/mL for 24 h. The MDA-MB-231 cells were placed in 96-well plates (5000 cells/well) and cultured with free medium, following which the cells were treated with 0, 2, 5, 10, 20, 40, 80, 100 µg/mL of free MNP MCM-41, BBR, BBR/MCM-41 and doxorubicin standard for 24 h at 37 ºC. Then the medium was discarded and the cells were treated with 0.1% MTT reagent and incubated for 4 h at 37 ºC. The formazan crystals so formed were solubilized in DMSO and the absorbance was noted immediately at 496 nm using a micro plate reader. Equivalent amounts of dimethyl sulfoxide (DMSO) were served as control for this experiment. The principle of MTT assay relates to quantifying the conversion of the tetrazolium compound into the formazan product using metabolically active viable cells.

$$\text{Viable cells (\%)} = \left(1 - \frac{\text{Number of purple coloured cells}}{\text{Number of total cells}}\right) \times 100$$

The percentage of inhibition of cell proliferation was calculated using the equation. IC_{50} is defined as the concentration required reducing the 100% cells to 50%. IC_{50} value was calculated and plotted curves using the below equation:

$$\text{Growth inhibition (\%)} = \frac{Abs_{zero} - Abs_{sample}}{Abs_{zero}} \times 100$$

RESULTS AND DISCUSSION

Drug response study: The prepared BBR/MNPs carried drug response study by the UV/Vis spectrum was reported to have a strong absorption band at 251 and 430 nm, which can be attributed to charge transfer and the extra framework of iron clusters on the silicas. Fig. 1 shown absorption peaks at 232, 266, 346, 403 and 428 nm have been reported to represent BBR. In present study, a broad peak observed at 210-607 nm can be assigned to the overlap of the Fe_2O_3 and BBR absorption bands. This result confirmed the surface interaction of iron nanoparticles and the drug on the surface of the silica materials.

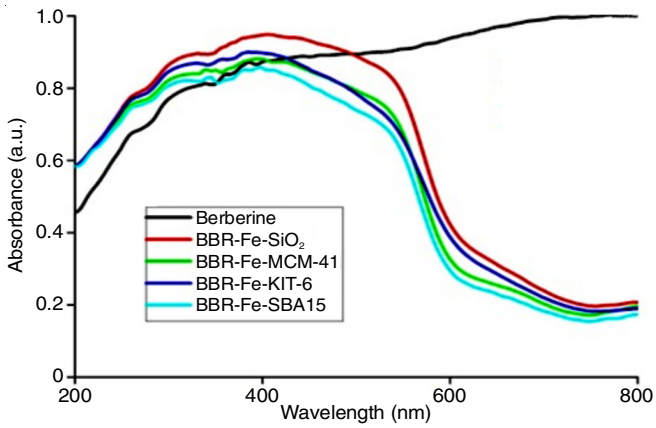

Fig. 1. Drug response study

FTIR: The BBR drug exhibited significant bands located at 3410 cm^{-1} that representing O–H stretching vibrations explaining the presence of water molecules on all materials. Other major bands expressed at 2922 and 2853 cm^{-1} indicated C–H stretches (alkanes). Similarly, peaks at 1646, 1140 and 1157 cm^{-1} corresponded to aromatic C=C vibrations, C-H bending in-plane and C–H vibrations, respectively. These major peaks were in line with the earlier report. In addition, two peaks at 577 and 709 cm^{-1} are attributed to stretching and bending vibration modes of the Fe–O in the Fe–O–Si bonds (Fig. 2).

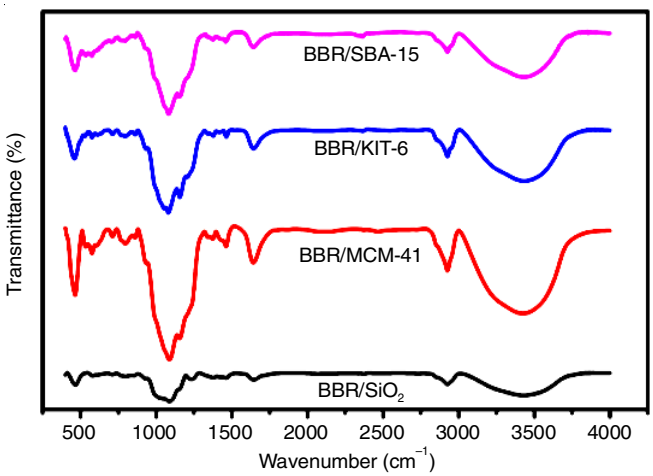

Fig. 2. FTIR spectrum of berberine loaded MNPs

X-ray diffraction (XRD): The peaks observed at 24.3º, 33.2º, 35.7º, 49.6º, 54.2º, 62.6º and 64.2º are due to Fe_2O_3 on the surface of the silica materials. The peaks observed at 14.9º, 18.2º, 41.0º are due to characteristic peaks of drug berberine present in all materials (Fig. 3). These results indicated the successful loading of the drug on all the materials (Fe-SiO_2, Fe-MCM-41, Fe-KIT-6 and Fe-SBA-15).

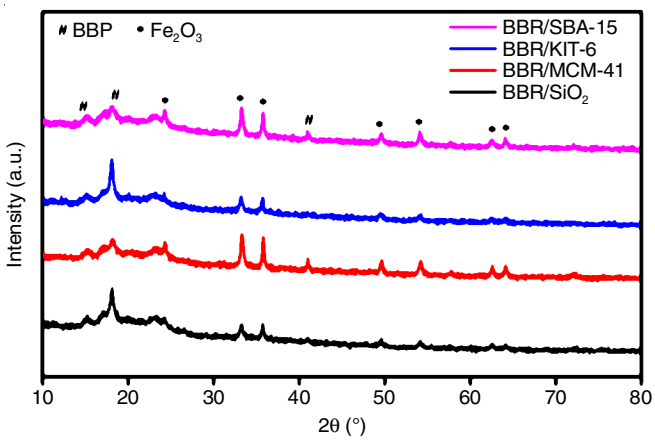

Fig. 3. XRD curves of berberine loaded MNPs

Thermal studies: TGA profiles of all materials shown in the Fig. 4 were reported showing two stages of weight loss observed at different temperatures. The initial weight loss observed below 200 ºC can be viewed as the removal of absorbed water from the material and the decomposition of drug from the material. The BBR drug has been reported to degrade between

200 and 250 ºC (Fig. 4). The weight loss between 250 and 750 ºC is due to dehydroxylation from the surface silanol group (Si-OH). Weight loss appears to be less with SBA-15 compared to all materials.

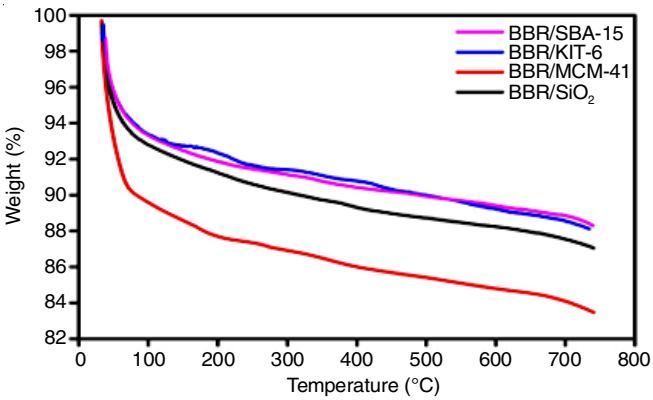

Fig. 4. TGA of BBR loaded MNPs

HRSEM studies: HRSEM images revealed that all the materials possess irregular shape, spherical like morphology which is due to the drug loading on the surface of the silica materials containing nanoparticles. SEM graphs of all MNPs before and after drug loading increased their diameter indicated clearly and its size range from 100-250 nm. Among all types of MNP, BBR/MCM-41 and BBR/SBA-15 possess the optimum size range with good in appearance (Fig. 5).

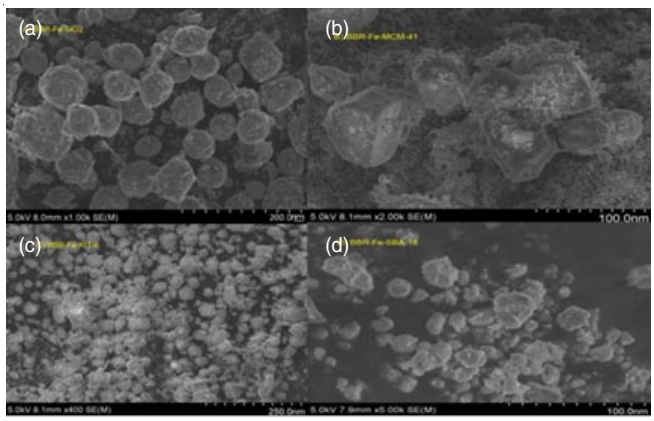

Fig. 5. HRSEM images of BBR loaded MNPs, (a) BBR/SiO_2, (b) BBR/MCM-41, (c) BBR/KIT-6, (d) BBR/SBA-15

Loading efficiency: Loading efficiency of all the prepared four berberine loaded MNPs were calculated. As indicated percentage of drug loaded was high to BBR/MCM-41 with 98% (Fig. 6). The other three MNPs were also in the range.

Colloidal stability: The colloidal stability analysis was conducted for 7 days using dynamic light scattering instrument at 37 ºC and determined. The percentage stability of berberine loaded magnetic nanoparticles was shown in Fig. 7.

Zeta potential (ζ): Measuring their zeta potential values at a pH from 3 to 11 for the electrostatic stabilization of nanoparticles was estimated. Indicated surplus negative charge of Fe-MCM-41 MNP might be due to presence of iron molecules on their surface. The final product, BBR/MCM-41 nanoparticles,

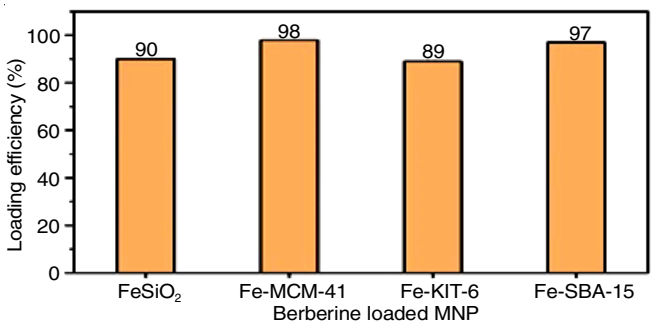

Fig. 6. Drug loading efficiency of formed MNPs

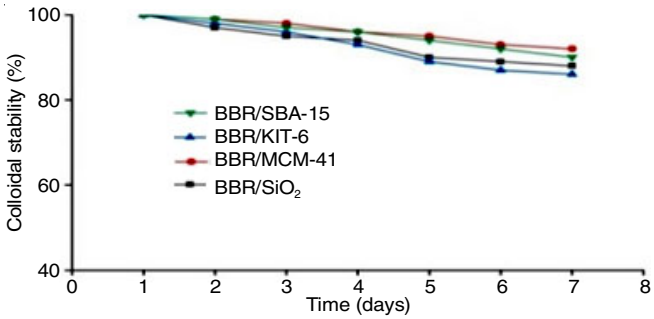

Fig. 7. Colloidal stability of loaded MNPs

possessed a positive charge due to its presence of drug named berberine on its surface (Fig. 8).

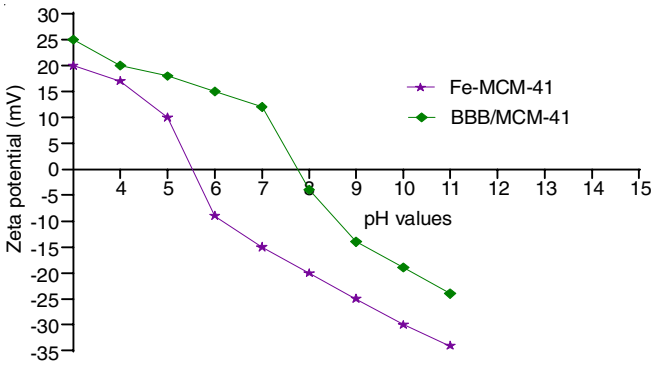

Fig. 8. Zeta potential study of Fe-MCM-41 and BBR/MCM-41 MNPs

Vibrating sample magnetometer (VSM) analysis: VSM gives the hysteresis curves for the magnetic nanoparticles. Among all four magnetic nanoparticles, Fe-MCM-41 MNPs before drug loading possessed an optimum particle size *i.e.*, 50 nm. Then, the VSM study was done for the Fe-MCM-41 MNP. The magnetization property of synthesized Fe-MCM-41 Magnetic nanoparticles was analyzed at 37 ºC (normal body temperature). The saturated magnetization (Ms) value of Fe-MCM-41 MNP was 81.76 emu/g, as obtained by vibrating sample magnetometer analyses. Zero remanence and coercivity was observed in the hysteresis loops, indicating that the synthesized Fe-MCM-41MNP was superparamagnetic. Superparamagnetic materials can be easily magnetized when exposed to a magnetic field and can be unmagnetized the field when the induced magnetic field is turned off. The prepared Fe-MCM-41 magnetic nanoparticles have a small core size *i.e.* 50 nm, has shown a magnetic behaviour with zero remanence

and coercivity values (Fig. 9). The synthesized MNPs in this study were proved to be super-paramagnetic. In the absence of an applied magnetic field, magnetic MNPs would not show any magnetic properties. This property is a desired characteristic in biomedical applications for several diseases. These magnetite Fe-MCM-41 magnetic nanoparticles, stabilized by the loading with drug named berberine. Loaded magnetic nanoparticles can be effectively used for diagnosis, imaging and for therapy owing to their low particle size with high surface area to volume ratio.

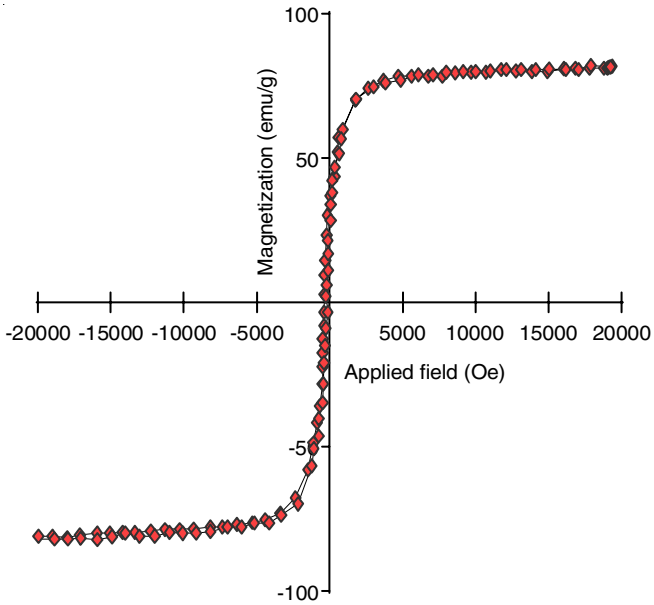

Fig. 9. Vibrating sample magnetometer analysis for Fe-MCM-41 MNP

Dissolution study: *In vitro* dissolution studies of all four types of MNPs at a three different pH 5.5, 6.5, 7.4 are shown in Fig. 10. At different pH 5.5, 6.5, 7.4, the % drug release of pure BBR results 34 ± 0.71, 32 ± 1.03, 30 ± 1.31, respectively. The proved formulation BBR/MCM-41MNP dissolution carried at phosphate buffer solutions pH 5.5, 6.5, 7.4 exhibited 86%, 84%, 82% of drug release at 36 h. This results indicated that the drug release was greater for BBR loaded MNPs than the pure BBR due to its nanosized particles with more surface area, which leads to more bioavailability. As the pH decreases the % of drug release increases. Hence, the acidic pH conditions are favourable.

***In vitro* cytotoxicity study of berberine loaded MCM-41 MNPs:** It is essential to evaluate the cytotoxic nature of formulated BBR/MCM-41MNP for their anticancer benefit(s). The cytotoxicity potential was determined by MTT assay method. The cytotoxic effects of standard doxorubicin, BBR, MCM-41 MNP and BBR/MCM-41 MNP were tested on breast cancer cells lines *i.e.*, MDA-MB-231 cells at 24 h incubation time. The MDA-MB-231 cells were treated to varying concentrations ranging from 0-100 µg/mL of standard doxorubicin, BBR, MCM-41 MNP and BBR/MCM-41 MNP for 24 h. In case of BBR treated cancer cells, the viability of cancer cells decreased sharply as concentration increases (0-100 µg/mL) (Fig. 11a). A similar result was seen with BBR/MCM-41 MNP at all tested concentrations. The MTT assay values exhibited a concentration based proliferative effect (0-100 µg/mL) by BBR and BBR/MCM-41 MNP formulations as seen in the study of % cell viability. IC_{50} value is the exact half inhibitory concentration (50% cell growth inhibitory concentration), (Fig. 11b) found to be 16.754 ± 0.651 with BBR, 6.750 ± 0.048 with BBR/MCM-41 MNP, 4.955 ± 0.042 with doxorubicin (STD drug) treatment. Table-1 showed that the BBR/MCM-41 MNP exhibited good inhibition upon MDA-MB-231 cells growth. Due to the targeted drug delivery, the increased inhibitory rate effected cell viability as shown in Fig. 11c. Using multiple variance analysis (one way ANOVA), the statistical analysis was performed with three number of replicates.

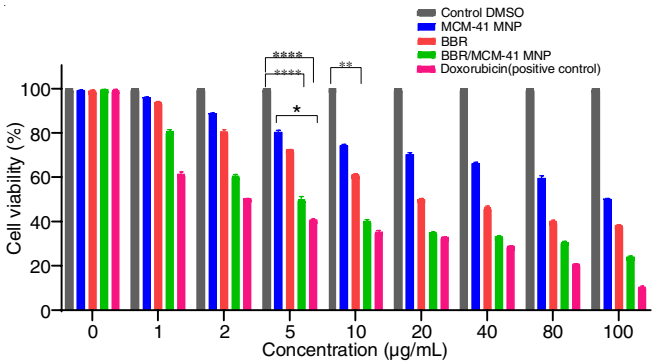

Fig. 11a. % Cell viability by MTT assay. The % cell viability of control DMSO, BBR, MCM-41 MNP, BBR/MCM-41 MNP and std. doxorubicin on treated MDA-MB 231 breast cancer cell lines at 24 h. Statistical analysis was performed using multiple variance analysis (one way ANOVA) (*$p < 0.01$, **$p < 0.01$, ****$p < 0.0001$, significant and n = 3)

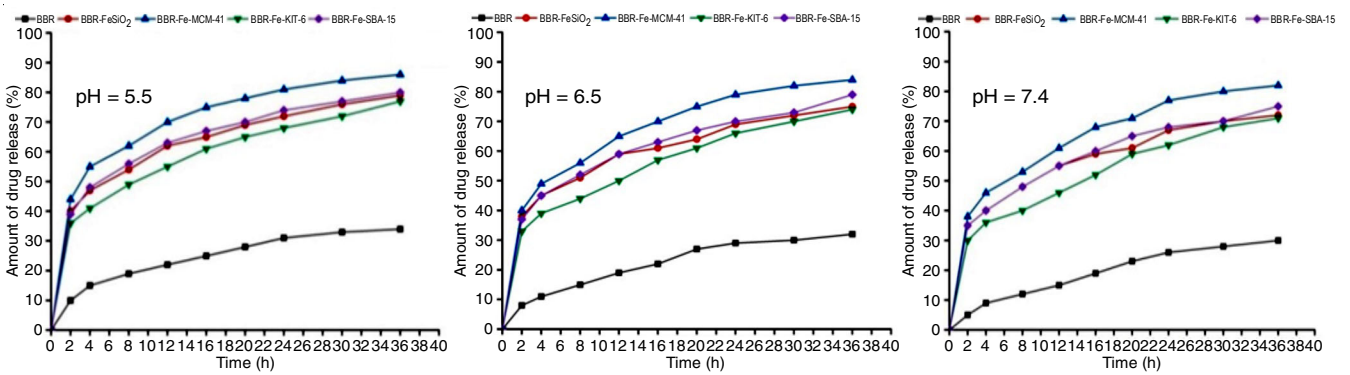

Fig. 10. *In vitro* dissolution study of BBR and BBR loaded MNPs at pH 5.5, 6.5, 7.4

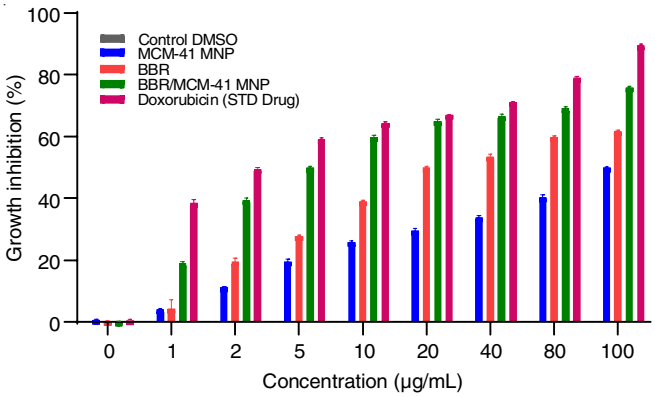

Fig. 11b. % Cell growth Inhibition calculated for control DMSO, BBR, MCM-41 MNP, BBR/MCM-41 MNP and std. doxorubicin on treated MDA-MB 231 breast cancer cell lines with mean ± SD

TABLE-1
IC_{50} VALUE BY MEAN ± SD VALUES

BBR	BBR/MCM-41 MNP	Doxorubicin (std. drug)
16.754 ± 0.651	6.750 ± 0.048	4.955 ± 0.042

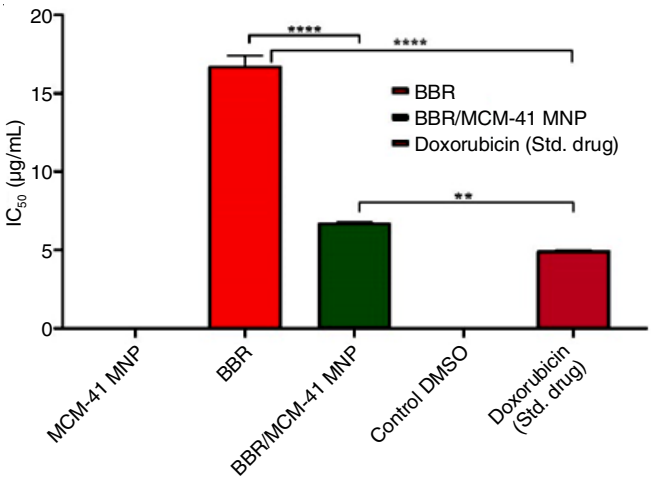

Fig. 11c. IC_{50} value calculated for control DMSO, BBR, MCM-41 MNP, BBR/MCM-41 MNP and std. doxorubicin on treated MDA-MB 231 breast cancer cell lines. Statistical analysis was performed using multiple variance analysis (one way ANOVA) (**$p < 0.02$ and ****$p < 0.0001$, significant and n = 3)

Conclusion

In present study, four berberine-loaded magnetic nanoparticles were prepared using modified co-precipitation methods with calcination. They were characterized by drug response study, FTIR, XRD, TGA, HRSEM, loading efficiency, colloidal stability, zeta potential, VSM and *in vitro* drug release study against time and *in vitro* cell line studies. The drug response study found that berberine had a maximum absorption at 403 nm. The resulting XRD showed that the formed composites retained an ordered mesoporous structure after the formation of iron oxide nanoparticles in the pores. FTIR indicated that the surface contains silanol groups and Fe-O on the surface of the materials at 1093 and 1020 cm^{-1} peaks, respectively. TGA indicated that BBR/KIT-6 MNPs was little more stable at different temperatures as it has shown less weight loss. Scanning electron microscopy (SEM) revealed that all the mesoporous magnetic nanoparticles are within the size range of 50 to 200 nm before loading and 100 to 250 nm after loading with berberine and also have a regular spherical shape. All four BBR containing MNPs with good loading efficiency and colloidal stability. The zeta potential of Fe-MCM-41 MNP was negatively charged; suggesting that the excess negative charge of Fe-MCM-41 nanoparticles could be due to the presence of iron molecules on its surface. The final product, BBR/MCM-41 MNP nanomaterial possesses a positive charge due to its presence of drug named berberine on its surface. The saturated magnetization (Ms) value of Fe-MCM-41 MNP (iron oxide MNP without drug) (81.76 emu/g) was obtained by VSM analyses. *In vitro* dissolution study of all four types of MNPs at three different pH 5.5, 6.5, 7.4 were reported, among all BBR/MCM-41MNP at three different pH 5.5, 6.5, 7.4 exhibited 86%, 84%, 82%, respectively. The synthesized magnetic nanoparticles revealed the potential anticancer activity tested in *in vitro* breast cancer cell lines *i.e.* MDA-MB 231 cells evaluated by means of MTT assay. The percentage cell viability and IC_{50} values of BBR, BBR/MCM-41 MNP and doxorubicin standard drug was calculated to 16.754 ± 0.651, 6.750 ± 0.048, 4.955 ± 0.042, respectively. All the data was obtained statistically with One-way Anova analysis at mean and S.D. with three number of replicates.

ACKNOWLEDGEMENTS

The authors are grateful to Sigma-Aldrich and Merck for providing the polymers and reagents with high grade quality. The authors also acknowledge the School of Pharmaceutical Sciences, VISTAS, Chennai and Ramani pharma, Hyderabad for providing research facilities. This work forms a part of Ph.D. thesis of A. Madhulatha.

CONFLICT OF INTEREST

The authors declare that there is no conflict of interests regarding the publication of this article.

REFERENCES

1. Z. Tao, A. Shi, C. Lu, T. Song, Z. Zhang and J. Zhao, *Cell Biochem. Biophys.*, **72**, 333 (2015); https://doi.org/10.1007/s12013-014-0459-6
2. S. Becker, *Int. J. Gynaecol. Obstet.*, **131**, 36 (2015); https://doi.org/10.1016/j.ijgo.2015.03.015
3. A.G. Waks and E.P. Winer, *JAMA*, **321**, 316 (2019); https://doi.org/10.1001/jama.2018.20751
4. M. Zubair, S. Wang and N. Ali, *Front. Pharmacol.*, **11**, 632079 (2021); https://doi.org/10.3389/fphar.2020.632079
5. M.R. Ataollahi, J. Sharifi, M.R. Paknahad and A. Paknahad, *J. Med. Sci. Life*, **8(Suppl. 4)**, 6 (2015).
6. X. Fang, J. Cao and A. Shen, *J. Drug Deliv. Sci. Technol.*, **57**, 101662 (2020); https://doi.org/10.1016/j.jddst.2020.101662
7. S.K.S. Kushwaha, A. Rastogi, A.K. Rai and S. Singh, *Int. J. Pharmtech. Res.*, **4**, 542 (2012).
8. N. Harbeck, F. Penault-Llorca, J. Cortes, M. Gnant, N. Houssami, P. Poortmans, K. Ruddy, J. Tsang and F. Cardoso, *Nat. Rev. Dis. Primers*, **5**, 66 (2019); https://doi.org/10.1038/s41572-019-0111-2
9. J.K. Patra, G. Das, L.F. Fraceto, E.V.R. Campos, M.P. Rodriguez-Torres, L.S. Acosta-Torres, L.A. Diaz-Torres, R. Grillo, M.K. Swamy, S. Sharma, S. Habtemariam and H.-S. Shin, *J. Nanobiotechnology*, **16**, 71 (2018); https://doi.org/10.1186/s12951-018-0392-8

10. S.F. Hasany, A. Rehman, R. Jose and I. Ahmed, *AIP Conf. Proc.*, **1502**, 298 (2012); https://doi.org/10.1063/1.4769153
11. T.K. Indira and P.K. Lakshmi, *Int. J. Pharm. Sci. Nanotechnol.*, **3**, 1035 (2010).
12. T. Guo, M. Lin, J. Huang, C. Zhou, W. Tian and H. Yu, *J. Nanomater.*, **2018**, 805147 (2018); https://doi.org/10.1155/2018/7805147
13. H. Majidzadeh, M. Araj-Khodaei, M. Ghaffari, M. Torbati, J. Ezzati Nazhad Dolatabadi and M.R. Hamblin, *Colloids Surf. B Biointerfaces*, **194**, 111188 (2020); https://doi.org/10.1016/j.colsurfb.2020.111188
14. E. Mirhadi, M. Rezaee and B. Malaekeh-Nikouei, *Biomed. Pharmacother.*, **104**, 465 (2018); https://doi.org/10.1016/j.biopha.2018.05.067
15. M. Javed Iqbal, C. Quispe, Z. Javed, H. Sadia, Q.R. Qadri, S. Raza, B. Salehi, N. Cruz-Martins, Z. Abdulwanis Mohamed, M. Sani Jaafaru, A.F. Abdull Razis and J. Sharifi-Rad, *Front. Mol. Biosci.*, **7**, 624494 (2021); https://doi.org/10.3389/fmolb.2020.624494
16. V. Purcar, V. Raditoiu, C. Nichita, A. Balan, A. Raditoiu, S. Caprarescu, F.M. Raduly, R. Manea, R. Somoghi, C.-A. Nicolae, I. Raut and L. Jecu, *Materials*, **14**, 2086 (2021); https://doi.org/10.3390/ma14082086
17. M.S. Yilmaz, Ö.D. Özdemir and S. Piskin, *Res. Chem. Intermed.*, **41**, 199 (2015); https://doi.org/10.1007/s11164-013-1182-4
18. X. Wang, Y. Zhang, W. Luo, A.A. Elzatahry, X. Cheng, A. Alghamdi, A.M. Abdullah, Y. Deng and D. Zhao, *Chem. Mater.*, **28**, 2356 (2016); https://doi.org/10.1021/acs.chemmater.6b00499
19. B. Zhou, C.Y. Li, N. Qi, M. Jiang, B. Wang and Z.Q. Chen, *Appl. Surf. Sci.*, **450**, 31 (2018); https://doi.org/10.1016/j.apsusc.2018.03.223
20. S.W. Song, K. Hidajat and S. Kawi, *Langmuir*, **21**, 9568 (2005); https://doi.org/10.1021/la051167e
21. R. Bhanumathi, M. Manivannan, R. Thangaraj and S. Kannan, *ACS Omega*, **3**, 8317 (2018); https://doi.org/10.1021/acsomega.7b01347
22. H. Štorkánová, S. Oreská, M. Špiritovic, B. Heømánková, K. Bubová, M. Komarc, K. Pavelka, J. Vencovský, J.H.W. Distler, L. Šenolt, R. Beèváø and M. Tomèík, *Sci. Rep.*, **11**, 1 (2021); https://doi.org/10.1038/s41598-020-79139-8
23. M.M. Yallapu, S.F. Othman, E.T. Curtis, N.A. Bauer, N. Chauhan and D. Kumar, *Int. J. Nanomedicine*, **7**, 1761 (2012); https://doi.org/10.2147/IJN.S29290
24. N.A. Razak, N. Abu, W.Y. Ho, N.R. Zamberi, S. Tan, N.B. Alitheen, K. Long and S.K. Yeap, *Sci. Rep.*, **9**, 1514 (2019); https://doi.org/10.1038/s41598-018-37796-w
25. K. El-Boubbou, R. Ali, S. Al-Humaid, A. Alhallaj, O.M. Lemine, M. Boudjelal and A. AlKushi, *Pharmaceutics*, **13**, 553 (2021); https://doi.org/10.3390/pharmaceutics13040553